

Phase Separation by Coupled Single-Crystal Growth and Polycrystalline Fingering in Al-Ge: Theory

S. Alexander,^(a) R. Bruinsma, and R. Hilfer

*Department of Physics and Solid State Science Center, University of California at Los Angeles,
Los Angeles, California 90024*

and

G. Deutscher and Y. Lereah

*Department of Condensed Matter Physics, School of Physics and Astronomy, Tel Aviv University,
Tel Aviv 69976, Israel*

(Received 26 May 1987)

We present a theory for a new mode of phase separation in thin layers of amorphous Al-Ge alloys. Phase separation and crystallization occur in colonies developing from Al nuclei. Their growth is controlled by diffusion of Ge inside crystalline Al, and by the nucleation and growth of Ge crystallites on the Al-Ge interface. The growth velocity is constant as a consequence of the interaction between the ramified Al-Ge interface and the smooth boundary of the colony with the amorphous phase. Diffusion occurs only in a narrow strip controlled by a length scale related to the width of the Ge dendrites. The length scale is controlled by competition between nucleation and growth of Ge crystallites.

PACS numbers: 68.55.-a

An unusual growth morphology was recently discovered by Deutscher and Lereah¹⁻³ in the phase separation of amorphous alloys of Al-Ge. When thin layers (≈ 600 Å) of the melt are quenched and subsequently reheated they observe the growth of symmetric, essentially round, "colonies" consisting of a branched, centered, dendritic structure of polycrystalline Ge with the rim and interstices made out of single-crystal Al. In most situations no new Al crystals appear inside the colony. The crystallization of Ge takes place on the Al-Ge interface through the nucleation and growth of many small crystallites. The outer boundary of the colony is relatively smooth and certainly not dendritic. The relative concentrations of Al and Ge in the colonies are those of the amorphous phase.

This growth mode, which has been called the "dense branching morphology,"² appears to be possible only for the growth of polycrystalline material. It is intermediate between diffusion-limited aggregation, where no crystallization takes place, and the dendritic growth of a single crystal from an impure melt. The experimental results are described in more detail in the previous Letter³ where they are compared with the predictions of the theoretical model which will be presented here. Our purpose is first to understand the general requirements for this form of pattern formation, and second to predict both the growth velocity and the characteristic length scales of the density profiles. We start with the first question.

Below the eutectic point, the separation of a binary alloy into its constituent phases requires nucleation and growth through diffusion of the pure crystalline phases. Typical growth morphologies (spinodal, lamellar, den-

dritic, or large single crystals) are selected by the competition between diffusive growth mechanisms and nucleation. Our description for the new growth morphology has three central features:

(a) The dominant diffusion process is the diffusion of atomic Ge through *crystalline* Al.

(b) Nucleation and growth of Ge crystals occur only at the interface between Al and Ge.

(c) The nucleation of Al crystals in the *amorphous* phase is much more frequent than that of Ge but still rare. It controls the initiation of new colonies.

Thus the scenario we envisage for solidification is a two-stage process: First a nucleus of single-crystal Al is formed in the amorphous phase. It contains in solution a relatively large concentration of Ge atoms which, in a second stage, precipitate inside the Al to form Ge crystallites. Diffusion of Ge atoms occurs only in a thin layer until the Ge atoms are absorbed by the ramified Al-Ge boundary. The essential phenomenological features of this model are, we believe, immediate consequences from the experimental findings and the known properties of Al-Ge alloys.

(1) The observed Ge pattern suggests dendritic surface growth which is typical for diffusion-limited growth.⁴ Since the Al-Ge interface is separated from the amorphous phase by the Al rim, the Ge atoms have to diffuse through single-crystal Al.

(2) The nucleation of Al in the amorphous phase must be much easier than that of Ge^{1,5} because at lower temperatures it is found that only Al crystallizes while the Ge is expelled into the amorphous phase without nucleation. As noted, we assume that the Al nucleation creates the colonies and that nucleation of Ge in the

amorphous phase can be neglected.

(3) Atomic diffusion in an amorphous phase is very slow compared with the crystalline phase. Note that this is certainly not true for a *melt* (and in that case we would also expect a capillary instability for the Al-melt interface).

Because the interface between Al and the amorphous phase is sharp (compared with the Al-Ge interface) we will ignore its microstructure and treat it according to continuum thermodynamics as follows. From the Al-Ge phase diagram⁶ (Fig. 1) it is evident that the equilibrium miscibility of Ge in Al at, say, 200°C is extremely low. However, crystallization of Ge at the boundary between Al and the amorphous phase is apparently rare, presumably because of a high nucleation barrier, and for the moment we will neglect it. Since it is of course the equilibrium with crystalline Ge which leads to the low miscibility, we can extend the solidus and liquidus lines below the eutectic (see Fig. 1). This gives a miscibility of $\approx 9\%$ Ge (c_L) for this quasiequilibrium phase of Al. If we assume that the Al-amorphous interface is in quasiequilibrium then we can equate c_L with the concentration of atomic Ge inside the Al at the boundary, in good agreement with experiment.³ This assumption entails that a (stable) liquid melt is a good description of the thermodynamics of the quenched amorphous phase. A similar argument also determines the concentration c_R of

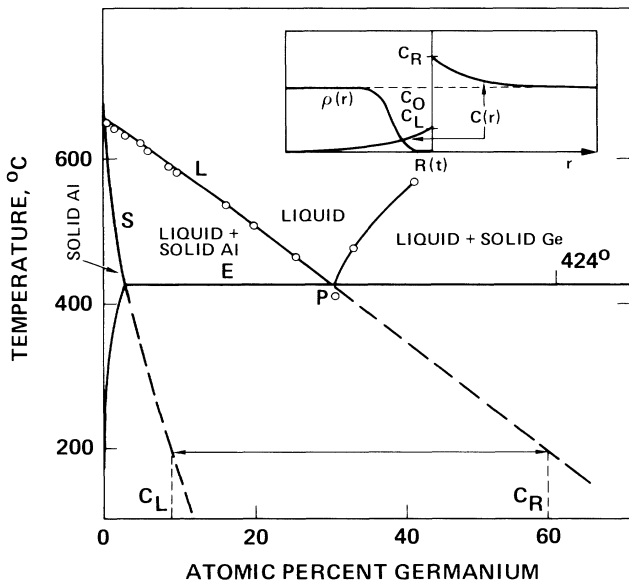


FIG. 1. Equilibrium phase diagram of Al-Ge. The liquidus is indicated by L, the solidus by S, the eutectic line by E, and the eutectic point by P. If we could prevent Ge solidification then the quasiequilibrium phase diagram would be obtained by extension of the liquidus and solidus below the eutectic. An alloy of concentration c_0 quenched from the melt below the eutectic would then phase separate into c_L and c_R . Inset: A typical ($\beta=500$, $\epsilon=0.001$) concentration profile for solid (g) and diffusing (f) Ge.

Ge on the other side of the boundary, in the amorphous phase (see Fig. 1). The Al-amorphous boundary does not suffer from capillary instabilities. The typical wavelength⁵ for such instabilities is of order $(d\xi)^{1/2}$ with d the capillary length ($\approx 1 \text{ \AA}$) and ξ the diffusive width of the interface (see below). Since in our case ξ is only of order $1 \mu\text{m}$, we can assume the Al-amorphous boundary to be flat.

We now turn to describe in an averaged fashion the Al-Ge interface which has a more complicated structure. Following Ball, Nauenberg, and Witten⁷ we replace the local concentration of atomic Ge by its radial average $c(r)$ and that of crystalline Ge by its radial average $\rho(r)$. To lowest order⁸ in ρ ,

$$\partial c/\partial t = D_L V^2 c - \partial \rho/\partial t \tag{1a}$$

on the "left" inside the Al and

$$\partial c/\partial t = D_R V^2 c \tag{1b}$$

on the "right" inside the amorphous phase, where D_L and D_R are the respective diffusion constants for Ge. At the boundary, one has $c = c_L$ on the Al side ($r = R_-$) and c_R on the amorphous side ($r = R_+$). We describe the growth process in its simplest form⁹:

$$\partial \rho/\partial t = Bc\rho \tag{2}$$

because new growth occurs only at Al-Ge interfaces. The phenomenological rate constant B describes the total Ge growth and therefore, implicitly, both the growth and the nucleation of the Ge crystallites. We shall discuss the physical relationship between B and the actual process of growth at the Ge-Al interfaces at a later stage. The most serious problem with Eq. (2) is that it is purely local: Inside the Al the ρ field can only grow where it already exists. We shall introduce the seeds for the growth through the boundary conditions at the outer (Al-amorphous) boundary $r = R(t)$.

The diffusion field must obey mass conservation:

$$\frac{d\{R(t)[\Delta c + \rho(R)]\}}{dt} = D_L \left. \frac{\partial c}{\partial r} \right|_{r=R_-} - D_R \left. \frac{\partial c}{\partial r} \right|_{r=R_+} \tag{3}$$

Here $\rho(R)$ is a small seed concentration of crystalline Ge at the boundary with the amorphous phase and $\Delta c = c_R - c_L$ is the discontinuity in the Ge concentration (miscibility gap) across the boundary. Steady-state solutions to Eqs. (1)-(3) are constant-velocity profiles:

$$c(r, t) = c_0 f(z), \tag{4a}$$

$$\rho(r, t) = c_0 g(z), \tag{4b}$$

where $R = vt$, $z = (r - vt)/\xi$, c_0 is the concentration of Ge in the amorphous phase, and $\xi = D_L/v$ is the basic length scale of the problem. The reason that only constant-velocity profiles are found is clear from Eq. (3): The ramified, crystalline Al-Ge interface near the boundary acts as a sink for diffusing Ge which causes a

finite value for the concentration gradient and thus a finite velocity. For sufficiently long times, i.e., $v^2t/D_L \gg 1$, the curvature of the interface can be neglected and we obtain

$$f' + f'' = -g', \quad (5a)$$

$$-g' = \beta fg, \quad (5b)$$

where $\beta = c_0 B D_L / v^2$ is a dimensionless parameter. Far to the left ($z \rightarrow -\infty$) we have $g=1$ ($\rho=c_0$) by mass conservation and $f=f'=0$. Therefore from Eq. (5)

$$g = 1 - f - f'. \quad (6)$$

At the Al-amorphous boundary ($z=0$) we have $f=c_L/c_0$ because $c(R=vt)=c_L$. Thus Eq. (6) relates $g(0) [= \rho(R)/c_0]$ to $f'(0)$. Using the solution of Eq. (1b)—the amorphous phase—in Eq. (3) with $f(+\infty)=1$, we find that Eq. (1b) is decoupled from the solution behind the front and that D_R is an irrelevant parameter. Substituting Eq. (6) into (5b) gives us a closed nonlinear equation for f with β as the only control parameter:

$$f' + f'' = \beta f(1 - f - f'). \quad (7)$$

Far inside the colony (z large and negative) f is small, and one can linearize Eq. (7) with solution $f \propto e^{z/\zeta}$ where

$$\zeta^{-1} = \frac{1}{2} [-1 + (1 + 4\beta)^{1/2}]. \quad (8)$$

It is most convenient to display the general solution as trajectories in the f - f' plane as shown in Fig. 2. The trajectories, which already fulfill the boundary conditions at $z = -\infty$, emerge from the origin with a slope $f'/f = 1/\zeta$. All trajectories end at the fixed point (1,0) on the f axis. The straight line $1 - f - f' = 0$ ($g=0$) is an exact solution of Eq. (7) and thus acts as a separatrix because flow

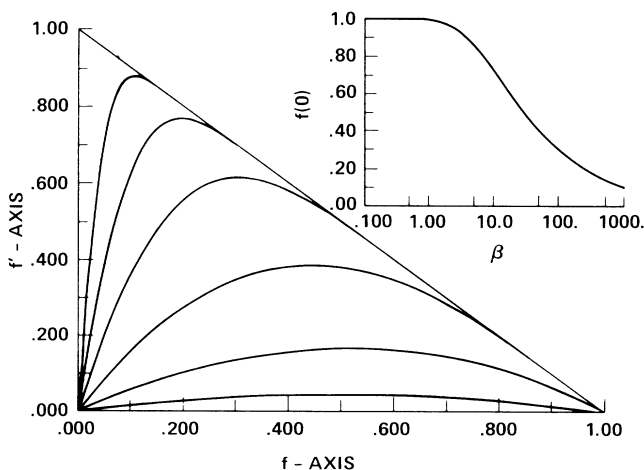


FIG. 2. Trajectories fulfilling the boundary conditions at $z = -\infty$ for selected values of β ($\beta=0.2, 1, 5, 25, 100$, and 500). Inset: Dependence of $f(0) = c_L/c_0$ on β for trajectories fulfilling the boundary conditions both at $z = -\infty$ and $z=0$ with a seed concentration $\epsilon = 10^{-3}$.

lines cannot cross. This means that one cannot have $g=0$ for $z \leq 0$. The low-velocity solutions ($\beta \geq 1$) are tangential to $g=0$ at (1,0) and approach it exponentially fast ($f''/f' \rightarrow -1$). The two boundary conditions on f at the boundary $z=0$ are

$$f(0) = c_L/c_0, \quad (9a)$$

$$1 - f(0) - f'(0) = \epsilon, \quad (9b)$$

where $\epsilon = g(0)$, the seed concentration. The second boundary condition [Eq. (9b)] determines a straight line parallel to the separatrix. If we choose a value for β we must follow the associated flow line starting from (0,0) until it intersects this straight line and read off the corresponding value $f(0) = c_L/c_0$. This determines β , and thus v , as a function of c_L (see the inset in Fig. 2). For $\beta \gg 1$, the flow line is practically a straight line up to $g = \epsilon$ so that, from Eq. (8), $f'(0)/f(0) \approx \beta^{1/2}$ and from Eq. (9b) and the definition of β ,

$$v \approx (c_L/c_0) D_L / \zeta \xi, \quad (10a)$$

$$\zeta \xi \approx (D_L/c_0 B)^{1/2}. \quad (10b)$$

Measuring the characteristic length scale $\zeta \xi$ from the density profile deep inside the colony (i.e., $z \rightarrow -\infty$) we can check Eq. (10a) since c_L , c_R , and D_L are known. If β changes from $\beta < 1$ to $\beta > 1$ one expects a qualitative change in the growth mode because for $\beta < 1$ (high velocity) and small ϵ only concentrations $c_L \approx c_0$ are possible, and conversely, β is a very sensitive function of c_L/c_0 near $c_L/c_0 = 1$ (see Fig. 2).

The parameter ϵ introduces nonlocality into the equations. In spite of the purely local form of Eq. (2) this is sufficient to assure continued growth, [i.e., solutions of Eq. (7)]. Physically it can originate in two ways: Either the growing tips "find" small crystallite Ge grains which have nucleated in the amorphous phase but are too small to be stable and grow on their own or crystals nucleated behind the boundary grow sufficiently rapidly to catch up. For small but finite ϵ the velocity selection is not very sensitive to ϵ . Thus for experimental value of c_L/c_0 (≈ 0.15) one finds $400 < \beta < 600$ for $10^{-4} < \epsilon < 10^{-3}$.

Although our predictions concerning the constant growth velocity and the relation between v and ξ seem to be confirmed by experiment, we did not really solve the problem of determining the velocity selected by the growing front. The reason is that the reaction rate B is not a material parameter: $B\rho$ is the capture rate for diffusing Ge by Al-Ge interfaces. The capture probability near the interface is expected to be high because of the very high supersaturation of Ge in the Al rim. Assuming the capture probability to be 1, we can estimate the capture rate from the time required to diffuse to the Al-Ge surface. This gives $Bc_0 \approx D_L/\xi_1^2$ where ξ_1 is a typical length for the texture, say the width of an Al "fjord." This, however, is only compatible with Eq. (10), the velocity selection, if ξ_1 is of order of ξ , i.e., if

the radial and angular Ge density profiles are governed by the same length scale. This reduces the determination of B to a search for a selection mechanism for the width of the Ge fingers. For that we need a more detailed model. Contrary to the normal situation for dendritic growth, we cannot determine this length from a simple competition between diffusion and surface tension in view of the considerable interfacial roughness.³ This roughness is related to the polycrystallinity of the Ge dendrites. In the fingers one observes a broad distribution of crystallite sizes with the largest comparable to the finger width ξ . This suggests that ξ is determined by a competition between the growth of an individual crystallite in a supersaturated atmosphere ($c = c_L$) and the screening due to the nucleation and growth of nearby crystallites with different crystallographic orientation. This mechanism for pattern formation is peculiar to the growth of polycrystalline materials and is quite distinct from both diffusion-limited aggregation and normal dendritic growth. We expect to present a detailed model along these lines separately.

We would like to thank A. Zangwill for useful discussions. We gratefully acknowledge financial support from the National Science Foundation under Grant No. 84-12898 and from the Deutsche Forschungsgemeinschaft.

^(a)Also at The Racah Institute of Physics, The Hebrew University, Jerusalem, Israel.

¹G. Deutscher and Y. Lareah, *Physica* (Amsterdam) **140A**, 191 (1986).

²E. Ben-Jacob, G. Deutscher, P. Garik, N. Goldenfeld, and Y. Lareah, *Phys. Rev. Lett.* **57**, 1903 (1986).

³G. Deutscher and Y. Lareah, preceding Letter [*Phys. Rev. Lett.* **60**, 1510 (1988)].

⁴Heat diffusion is much faster than atomic diffusion and can be ignored.

⁵J. Langer, *Rev. Mod. Phys.* **52**, 1 (1980). The capillary instability is also suppressed by a gap v/ξ in the capillary wave spectrum. If instead of an amorphous alloy we were to have a melt across the boundary, then the diffusive width of the boundary could be macroscopic and capillary instabilities would be important.

⁶M. Hansen, *Constitution of Binary Alloys* (McGraw-Hill, New York, 1958), p. 97.

⁷R. Ball, M. Nauenberg, and T. A. Witten, *Phys. Rev. A* **29**, 2017 (1984).

⁸It would be more accurate to take into account the excluded-volume effects implied by the presence of solid Ge explicitly in Eqs. (1a) and (1b). This replaces $\partial^2 c / \partial r^2$ by $(\partial/\partial r)(1-\rho)(\partial/\partial r)[c/(1-\rho)]$ and $c\rho$ by $c\rho/(1-\rho)$. These changes somewhat complicate the analysis but do not change its essential features.

⁹Nonlinear correction terms in ρ can be neglected in Eq. (2) because $c\rho$ is only appreciable near the rim where ρ is small compared to 1. Adding a term $cV^2\rho$ on the right-hand side of Eq. (2), as in Ref. 8, did not affect our results and is not adequate to represent nonlocality. More serious is the neglect of terms of the form $A(\nabla\rho)^2$ as they lead to qualitative changes in the flow lines. In the worst case ($A \sim \xi^2/c_0$) this would restrict us to $\beta < 50$.